Investigation of the Photophysical and Electrochemical Properties of Alkoxy-Substituted Arylene−Ethynylene/Arylene−Vinylene Hybrid Polymers

Daniel Ayuk Mbi Egbe,* Bader Cornelia, Jürgen Nowotny, Wolfgang Günther, and Elisabeth Klemm*

Institut für Organische Chemie und Makromolekulare Chemie der Friedrich-Schiller-Universität Jena, Lessingstrasse 8, D-07743 Jena, Germany

Received February 24, 2003; Revised Manuscript Received April 22, 2003

ABSTRACT: High-molecular-weight, soluble and thermostable alkoxy-substituted arylene−ethynylene/arylene−vinylene conjugated polymers, **13** and **14**, have been successfully synthesized through the Horner−Wadsworth−Emmons olefination of luminophoric dialdehydes **7** and **9** and bisphosphonate **12** in very good yields. They were characterized through ^{1}H NMR, ^{13}C NMR, IR, and elemental analysis. The investigation of their photophysical and electrochemical properties has been carried out. Although almost identical absorption and emission spectra were obtained in dilute chloroform solution for all polymers **13**, the full width at half-maximum (fwhm) value of the emission curves depends on the length of the attached side chains. The presence of anthracenylene units in **14** leads to a red shift of its absorption and emission spectra relative to **13**. Strong self-reabsorption after excitation in solution was observed for this polymer. The solid-state photophysical properties of **13** and **14** (photoconductivity, absorption and emission spectra, fluorescence quantum yield, Stokes shift, and fwhm) greatly depend on the *nature* (linear or branched), *length*, and *location* of the grafted alkoxy side groups. Photoconductivity is easily detected in polymers having octadecyloxy chains (**13aa**, **13ab**, **14**). Long linear (octadecyl, i.e., **13aa**) or short branched (2-ethylhexyl, i.e., **13cc**) side chains at position R_2 (phenylene−vinylene segment) are necessary to obtain sharp and well-resolved emission spectra accompanied by high fluorescence quantum yields. The quasi-donor (phenylene−vinylene segment)−acceptor (arylene−ethynylene segment) nature of these polymers could explain the great discrepancy between the electrochemical band gap energy, $E_g^{ec} \approx 1.60$ eV, as obtained from the onset values of the redox potentials in cyclic voltammetry and in differential pulse polarography measurements, and the optical band gap energy, $E_g^{opt} \approx 2.30$ eV, from the absorption spectra.

Introduction

Since the past three decades, much attention has been focused on the investigation of the properties of π-conjugated polymers, culminating with the award of the Nobel Prize in chemistry in the year 2000 to Alan J. Heeger, Alan G. MacDiarmid, and Hideki Shirakawa for the discovery and development of conductive polymers.[1−5] Among semiconducting polymers, poly(phenylenevinylene)s (PPV) have been most widely studied since the discovery of electroluminescence in PPV by the group of Cambridge in 1990.[6] PPV's are good hole transporting materials but poor electron transporters. The need for materials with approximately balanced hole- and electron-transporting properties, which is a precondition for obtaining light-emitting-diode (LED) devices with high electroluminescence efficiencies, prompted many research groups to design and synthesize PPV derivatives with increased electron affinity, such as cyano-substituted PPVs,[7−10] trifluoromethyl-substituted PPVs,[11] oxadiazole-substituted PPVs,[12] and pyridine-containing PPVs.[13] A recent approach to increase the electron uptake of PPVs, which has been reported by our group[14] and others,[15] is to insert the electron-withdrawing acetylene (−C≡C−) into the PPV backbone, leading to hybrid poly(phenylene−vinylene)/poly(phenylene−ethynylene) (PPV/PPE) polymers.

* Corresponding authors: e-mail c5ayda@uni-jena.de or c9klel@rz.uni-jena.de.

Polymers **13aa** ($R_1 = R_2 =$ octadecyl) and **13ab** ($R_1 =$ octadecyl, $R_2 =$ octyl) were reported in one of our previous articles,[14c] in which we described the effects of alkoxy side chains in the photophysical properties of these polymers. In this report we extend the study of the side chains effects to polymers **13bb** ($R_1 = R_2 =$ octyl) and **13cc** ($R_1 = R_2 =$ 2-ethyhexyl) in order to make a clear and conclusive assertion about their influence on the properties on this class of compounds. Our synthetic strategy enables us to also obtain low band gap and defect-free polymer **14** by incorporating anthracenylene units into the polymer backbone. Polymers with low optical band gap energy and high absorption coefficient are of great interest for the design of organic photovoltaic cells.[16a] We attached long octadecyloxy side chains in **14** in order to confirm the fact that long side chains are needed for the easy detection of photoconductivity in this class of compounds.[14c] The good photoconductive behavior, the high fluorescence quantum yields in thin films, and the high absorption coefficients, ϵ_{max}, around 100 000 M^{-1} cm^{-1} of these polymers make them potential candidate for design of organic light-emitting diodes and organic photovoltaic devices.

To fit the energetic scheme of a photovoltaic device, it is necessary to determine through electrochemistry the energy levels of the valence band (HOMO) and the conduction band (LUMO) and the width of the gap between the bands of each component.[16] The energy gap between the bands can moreover be easily determined

10.1021/ma0301395 CCC: $25.00
Published on Web 06/28/2003

with the absorption spectroscopy. In this work the electrochemical behavior of polymers **13** and **14** and their corresponding monomers **7** and **9** has been investigated through cyclic voltammetry and differential pulse polarography. Their HOMO and LUMO energy levels have been estimated. A comparison between their electrochemical energy band gap, E_g^{ec}, and their optical energy band gap, E_g^{opt}, has been carried out.

Experimental Section

Instrumentation. ^{1}H NMR and ^{13}C NMR spectra were obtained in deuterated chloroform using a Bruker DRX 400 and a Bruker AC 250. Chemical shifts (δ values) are given in parts per million with tetramethylsilane as an internal standard. Elemental analysis was measured on a CHNS-932 Automat Leco. Infrared spectroscopy was recorded on a Nicolet Impact 400. A homemade apparatus served for the thermogravimetric measurements. Differential scanning calorimetry (DSC) was obtained with a Perkin-Elmer DSC 2C while heating or cooling at a rate of 10 °C/min. Mass spectroscopy was performed by chemical ionization with H_2O vapor as gas on a Finnigan Mat SSQ 710. Gel permeation chromatography (GPC) was performed on a set of Knauer using THF as eluent and polystyrene as a standard. The absorption spectra were recorded in dilute chloroform solution (10^{-5}−10^{-6} M) on a Perkin-Elmer UV/vis−NIR spectrometer Lambda 19. Quantum-corrected emission spectra were measured in dilute chloroform solution (10^{-6} M) with an LS 50 luminescence spectrometer (Perkin-Elmer). Photoluminescence quantum yields were calculated according to Demas and Crosby[17] against quinine sulfate in 0.1 N sulfuric acid as a standard (ϕ_{fl} = 55%). The solid-state absorption and emission were measured with a Hitachi F-4500. The films were cast from chlorobenzene. The quantum yield in the solid state was determined against a CF_3P−PPV (poly{1,4-phenylene-[1-(4-trifluoromethylphenyl)ethenylene]-2,5-dimethoxy-1,4-phenylene-[2-(4-trifluoromethylphenyl)ethenylene]}) copolymer reference that has been measured by integrating sphere as 0.43.[18] Electrochemical measurements (cyclic voltammetry and differential pulse polarography) were carried with a Princeton Research PAR 273 A [Pt disk electrode, dichloromethane, tetrabutylammonium hexafluorophosphate (Bu_4NPF_6), concentration 10^{-3} M, sweep rate 0.02 V/s (differential pulse polarography), 0.167 V/s (cyclic voltammetry)].

Materials. All starting materials were purchased from commercial suppliers (Fluka, Merck, and Aldrich). Toluene, tetrahydrofuran, and diethyl ether were dried and distilled over sodium and benzophenone. Diisopropylamine was dried over KOH and distilled. If not otherwise specified, the solvents were degassed by sparkling with argon or nitrogen 1 h prior to use. 1,4-Dibromo-2,5-dioctyloxybenzene (**1**),[19] 1,4-diethynyl-2,5-dioctyloxybenzene (**5**),[19] 2,5-dialkoxy-*p*-xylylenebis(diethylphosphonate)s (**12**),[14] 4-diiodo-2,5-di(2-ethyl)hexyloxybenzene (**6**),[14c,20] and 9,10-dibromoanthracene[21] were prepared according to known literature procedures.

1-Bromo-4-formyl-2,5-dioctyloxybenzene (**2**). To a solution of 1,4-dibromo-2,5-dioctyloxybenzene (**1**)[19] (4.9 g, 10 mmol) in diethyl ether (150 mL), cooled at 10 °C and kept under argon, was added a solution of butyllithium (2.7 M in heptane, 3.75 mL, 10 mmol). After 15 min, DMF (0.96 mL, 12.5 mmol) was added to the mixture, while the temperature was allowed to rise to 15 °C. The clear solution was kept between 10 and 15 °C and was stirred for 1.5 h. A 10% aqueous HCl solution (50 mL) was subsequently added to the mixture, and the phases were separated. The organic phase was washed with a $NaHCO_3$ solution and dried over $CaCl_2$. Diethyl ether was then distilled off, and the residue was chromatographed on a silica gel with a mixture of toluene/hexane (2/1) as eluent. **2** was obtained at R_f = 0.70 (3.3 g, 74.6%) as light yellow crystals. Mp: 58.2−58.9 °C. ^{1}H NMR (250 MHz, $CDCl_3$): δ/ppm = 0.83 → 1.86 ($CH_3(CH_2)_6$−), 3.82 → 4.03 (−CH_2O−), 6.76 → 7.29 (C_{aryl}−H), 10.39 (CHO). ^{13}C NMR (62 MHz, $CDCl_3$): δ/ppm = 14. 45, 14.46, 23.02, 26.31, 26.37, 29.39, 29.44, 29.58, 29.62, 32.14, 32.16 ($CH_3(CH_2)_6$−), 69.85 and 70.22 (−CH_2O−), 111.01 and 118.84 (−C_{aryl}−H), 121.34 (−C_{aryl}−Br), 124.65 (−C_{aryl}−CHO), 150.24 and 156.15 (C_{aryl}−OR), 189.33 (−CHO). Anal. Calcd for $C_{23}H_{37}BrO_3$ (441.46): C, 62.57; H, 8.44; Br, 18.09. Found: C, 62.68; H, 8.55; Br, 18.40.

2,5-Dioctyloxy-4-trimethylsilylethynylbenzaldehyde (**3**). 4-Bromo-2,5-dioctyloxybenzaldehyde (**2**) (3 g, 6.8 mmol), Pd(PPh_3)$_2Cl_2$ (105 mg, 0.15 mmol), and CuI (31.8 mg, 0.16 mmol) were added to a degassed solution of diisopropylamine (75 mL). Trimethylsilylacetylene (670 mg, 6.8 mmol) was added slowly and dropwise to the vigorously stirred suspension. The reaction mixture was then stirred at reflux for 8 h. After cooling, the white ammonium bromide precipitate was filtered off. The solvent was removed under reduced pressure, and the residue was chromatographed over a silica gel column with toluene as eluent. 2.6 g (84%, R_f = 0.83) of a dark yellow oil was obtained, which crystallizes when kept under 4 °C for weeks. ^{1}H NMR (250 MHz, $CDCl_3$): δ/ppm = 0.08 (−$Si(CH_3)_3$), 0.67 → 1.63 (−$(CH_2)_6CH_3$), 3.80 (−CH_2O−), 6.69 and 7.03 (−C_{aryl}−H), 10.28 (−CHO). ^{13}C NMR (62 MHz, $CDCl_3$): δ/ppm = 0.11 (−$Si(CH_3)_3$), 14.23, 22.80, 22.82, 26.19, 29.30, 29.36, 29.39, 29.45, 29.53, 31.94, 32.00 ($CH_3(CH_2)_6$−), 69.42 (−CH_2O−), 100.64 and 103.13 (−C≡C−), 110.10 and 118.00 (C_{aryl}−H), 120.30 (C_{aryl}−C≡), 125.24 (C_{aryl}−CHO), 154.39 and 155.53 (C_{aryl}−OR), 189.37 (−CHO).

4-Ethynyl-2,5-dioctyloxybenzaldehyde (**4**). Methanol (28 mL) and aqueous KOH (4 mL, 10%) were added at room temperature to a stirred solution of **3** (2.5 g, 5.4 mmol) in 55 mL of THF. The reaction mixture was then stirred 3 h at room temperature. The solvent was removed on a rotatory evaporator, and the residue was chromatographed on a silica gel column with toluene as eluent. Thus, 1.3 g (65%, R_f = 0.77) of a yellow substance was obtained. Mp: 116−117 °C. ^{1}H NMR (250 MHz, $CDCl_3$): δ/ppm = 0.88 → 1.86 (30H, m, $CH_3(CH_2)_6$−), 3.47 (1H, s, −C≡C−H), 4.04 (4H, t, ^3J = 6.5 Hz, −CH_2O−), 7.09 (1H, s, C_{aryl}−H), 7.31 (1H, s, C_{aryl}−H), 10.45 (1H, s, −CHO). ^{13}C NMR (62.9 MHz, $CDCl_3$): δ/ppm = 14.44, 23.02, 26.27, 26.40, 29.40, 29.50, 29.58, 29.65, 32.16 ($CH_3(CH_2)_6$−), 69.67 and 69.82 (−CH_2O−), 79.84, 84.93 (−C≡C−), 110.45 and 118.79 (C_{aryl}−H), 119.40 (C_{aryl}−C≡), 125.76 (C_{aryl}−CHO), 154.61 and 155.64 (C_{aryl}−OR), 189.49 (−CHO). IR (KBr): 3346 (w, −C≡C−H), 2924 and 2853 (vs, −CH_2− and −CH_3), 2760 (w, −CHO), 1683 (vs, −CHO), 1600 (s, phenyl ring), 1218 (C_{aryl}−OR) cm^{-1}. UV−vis ($CHCl_3$, 4.4 × 10^{-5} M): λ_{max}/nm (ϵ/(L mol^{-1} cm^{-1})), 268 (9800), 300 (13 700), 315 (13 000), 340 (11 250), 411 (17 000). Anal. Calcd for $C_{25}H_{38}O_3$ (386.57): C, 77.67; H, 9.90. Found: C, 77.39; H, 9.77.

1,4-Bis(4-formyl-2,5-dioctyloxyphenylethynyl)-2,5-dioctyloxybenzene (**7b**). 1,4-Diethynyl-2,5-dioctyloxybenzene (**5**)[19] (2.0 g, 5.58 mmol), 1-bromo-4-formyl-2,5-dioctyloxybenzene (**2**) (5.30 g, 12 mmol), Pd(PPh_3)$_4$ (242 mg, 0.209 mmol, 4 mol %), and CuI (43.3 mg, 0.209 mmol, 4 mol %) were added to a degassed solution of 35 mL of diisopropylamine and 80 mL of toluene. The reaction was heated at 70 to 80 °C for 24 h. After being cooled to room temperature, the ammonium bromide salt was filtered off; the filtrate was evaporated to around 30 mL and was added dropwise into 500 mL of vigorously stirred methanol. The precipitate was collected and chromatographed on silica gel column with toluene as eluent. Yield: 4.2 g (69%). Mp: 85−86 °C. MS (70 eV, ESI in H_2O): m/z = 1104 (M^+ + 1, 100%), 992 (20%), 880 (10%). ^{1}H NMR (250 MHz, $CDCl_3$): δ/ppm = 0.79 → 1.83 (90H, m, $CH_3(CH_2)_6$−), 3.93 → 4.01(12H, m, −CH_2O−), 6.95 (2H, s, C_{phenyl}−H), 7.03 (2H, s, C_{phenyl}−H), 7.25 (2H, s, C_{phenyl}−H), 10.37 (2H, s, −CHO).^{13}C NMR (62.9 MHz, $CDCl_3$): δ/ppm = 14.47 (CH_3−), 23.05, 26.34, 26.41, 26.48, 29.58, 29.61, 29.70, 29.76, 29.81, 32.18, 32.23 (−$(CH_2)_6$−), 69.62, 69.91, 70.09 (−CH_2O−), 91.58, 94.19 (−C≡C−), 110.48, 114.73, 117.73, 117.93, 121.07, 125.29, 153.97, 154.07, 155.90 (C_{phenyl}'s), 189.55 (−CHO). IR (KBr): 2926 and 2855 (vs, −CH_2− and CH_3−), 2755(w, −CHO), 2203 (w, disubst −C≡C−), 1681 (s, −CHO), 1601 (s, −C=C_{phenyl}−), 1287 and 1207 (s, C_{phenyl}−OR) cm^{-1}. UV−vis ($CHCl_3$, 1.8 × 10^{-5} M): λ_{max}/nm (ϵ/(L mol^{-1} cm^{-1})) 288.0 (22 930), 328.8 (28 600), 423.2 (57 060). Anal. Calcd for $C_{72}H_{110}O_8$ (1103.66): C, 78.36; H, 10.05. Found: C, 78.72; H, 9.55.

1,4-Bis(4-formyl-2,5-dioctyloxyphenylethynyl)-2,5-di(2-ethyl)-hexyloxybenzene **(7c)**. 1-Ethynyl-4-formyl-2,5-dioctyloxybenzene (**4**) (1.6 g, 4.14 mmol), 1,4-diiodo-2,5-bis(2-ethylhexyloxy)-benzene (**6**)[14c,20] (1.155 g, 1.97 mmol), $Pd(PPh_3)_4$ (91 mg, 0.079 mmol, 4 mol %), and CuI (15 mg, 0.079 mmol, 4 mol %) were given to a degassed solution of 15 mL of diisopropylamine and 45 mL of tetrahydrofuran. The reaction mixture was heated at 65−70 °C for 22 h. The ammonium iodide precipitate was filtered off after cooling to room temperature; the solvent was removed under reduced pressure. The residue was collected and chromatographed on a silica gel column with toluene as eluent. The desired product **7c** was obtained at $R_f = 0.36$ (1.2 g, 55%) alongside 1,4-bis[(4-formyl-2,5-dioctyloxy)phenyl)]but-1,3-diyne (**15**) at $R_f = 0.52$ (100 mg, 6.8%).

7c: Mp: 69−72 °C. MS (70 eV, ESI with H_2O): $m/z = 1104$ (M^+, 100%), 992 (50%). ^{1}H NMR (250 MHz, $CDCl_3$): δ/ppm = 0.79−1.81 (90H, m, alkyl side groups), 3.84 (4H, d, $^3J = 5$ Hz, $-CH_2O-$ ethylhexyl), 3.97 (8H, m, $-CH_2O-$ octyl), 6.94 (2H, s, $C_{phenyl}-H$), 7.03 (2H, s, $C_{phenyl}-H$), 7.26, (2H, s, $C_{phenyl}-H$), 10.38 (2H, s, −CHO). ^{13}C NMR (62.90 MHz, $CDCl_3$): δ/ppm = 11.91 (C_b), 14.71 (C_c), 23.29, 23.72, 24.68, 26.59, 26.70, 29.77, 29.83, 29.86, 29.93, 29.98, 31.27, 32.44, 32.46 ($-CH_2-$), 40.21 (C_a), 69.86, 70.07, 72.54, ($-CH_2O-$), 91.75, 94.53 ($-C\equiv C-$), 110.81 (C_3), 114.89 (C_{12}), 117.51 (C_6), 118.15 (C_{13}), 121.47 (C_5), 125.53 (C_2), 154.20, 154.55, 156.16 ($C_{phenyl}-OR$), 189.78 (−CHO). IR (FTIR): 2922 and 2854 (vs, $-CH_2-$ and CH_3-), 2753 (vw, −CHO), 2213 (vw, disubst $-C\equiv C-$), 1679 (vs, −CHO), 1600 (s, $-C=C_{phenyl}-$), 1207 (vs, $C_{aryl}-OR$) cm^{-1}. UV−vis ($CHCl_3$, 1.1×10^{-5} M): λ_{max}/nm (ϵ/(L mol^{-1} cm^{-1})) 329 (28 200), 428 (51 300). Anal. Calcd for $C_{48}H_{74}O_6$ (1103.66): C, 78.36; H, 10.04. Found: C, 77.92; H, 9.84.

15: Mp: 96−102 °C. MS (70 eV, ESI with H_2O): $m/z = 771$ (M^+, 60%), 363 (100%), 93 (100%). ^{1}H NMR (250 MHz, $CDCl_3$): δ/ppm = 0.78 → 1.81 (60H, m, $CH_3(CH_2)_6-$), 3.92 → 3.98 (8H, m, $-CH_2O-$), 6.92 (2H, s, $C_{phenyl}-H$), 7.23 (2H, s, $C_{phenyl}-H$), 10.37 (−CHO). ^{13}C NMR (62 MHz, $CDCl_3$): δ/ppm = 13.06, 21.64, 24.88, 25.01, 27.96, 28.09, 28.18, 28.22, 28.26, 30.77 ($CH_3(CH_2)_6-$), 68.30, 68.55 ($-CH_2O-$), 78.77 and 79.90 ($-C\equiv C-C\equiv C-$), 109.11, 117.39, 117.59 ($C_{phenyl}-H$), 124.71, 127.20, 128.01 ($C_{phenyl}-C$) 154.02, 154.18($C_{phenyl}-OR$), 188.03 (−CHO). IR (KBr): 2926 and 2855 (vs, $-CH_2-$ and CH_3-), 2759 (w, −CHO), 2209 and 2100 (vw, $-C\equiv C-C\equiv C-$), 1683 (vs, −CHO), 1600 (s, $-C=C_{phenyl}-$), 1286 and 1218 ($C_{phenyl}-$OR) UV−vis ($CHCl_3$, 2.0×10^{-5} M): λ_{max}/nm (ϵ/(L mol^{-1} cm^{-1})) 300 (24 280), 314 (23 000), 340 (20 200), 411.2 (31 000). Anal. Calcd for $C_{50}H_{74}O_6$ (771.13): C, 77.88; H, 9.67. Found: C, 77.03; H, 9.56.

9,10-Bis[(4-formyl-2,5-dioctyloxy)phenylethynyl]anthracene (**9**). 9,10-Dibromoanthracene (**8**) (470 mg, 1.39 mmol), 4-ethynyl-2,5-dioctyloxybenzaldehyde (**4**) (1.108 g, 2.866 mmol), $Pd(PPh_3)_4$ (65 mg, 5.59×10^{-2} mmol, 4 mol %), and CuI (11 mg, 5.59×10^{-2} mmol, 4 mol %) were given to a degassed solution of 20 mL of diisopropylamine and 50 mL of toluene. The reaction mixture was heated at 70−80 °C for 24 h in an argon atmosphere. After cooling to room temperature, the precipitated diisopropylammonium bromide was filtered off and the solvent was distilled off under vacuum. The residue was chromatographed on a silica gel column with toluene as eluent. 800 mg ($R_f = 0.64$, 60.53%) of a red substance was obtained. Mp = 138−142 °C. MS (70 eV ESI with H_2O): m/z = 947 ($M^+ + 1$, 100%), 835 (10%), 535 (5%), 158 (30%). ^{1}H NMR (400 MHz, $CDCl_3$): δ/ppm = 0.79 → 1.87 (30H, m, $CH_3(CH_2)_6-$), 4.13 (8H, t, $^3J = 6.46$ Hz, $-CH_2O-$), 7.26 (2H, s, $C_{phenyl}-H$), 7.38 (2H, s, $C_{phenyl}-H$), 7.62 (4H, d, $^3J = 9.88$ Hz, $C_{anthracenyl}-H$), 8.78 (4H, d, $^3J = 9.88$ Hz, $C_{anthracenyl}-H$), 10.48 (2H, s, CHO). ^{13}C NMR (100 MHz, $CDCl_3$): δ/ppm = 14.07 (CH_3-), 22.59, 22.64, 26.04, 26.10, 29.22, 29.33, 29.42, 29.52, 31.76, 31,79 ($-(CH_2)_6-$), 69.35 and 69.47 ($-CH_2O-$), 94.61 and 99.04 ($-C\equiv C-$), 109.36 and 117.04 ($C_{phenyl}-H$), 118.88 ($C_{phenyl}-C\equiv C-$), 120.21 ($C_{anthracenyl}-C\equiv C-$), 125.15 ($C_{phenyl}-CHO$), 126.92 and 132.25 ($C_{anthracenyl}-H$), 127.44 ($C_{anthracenyl}-C=$), 154.01 and 155.60 ($C_{phenyl}-OR$), 189.11 (−CHO). IR (KBr): 3056 (w, $C_{phenyl}-H$) 2929 and 2856 (vs, CH_2 and CH_3), 2756 (w, CHO), 2188 (w, disubst $-C\equiv C-$), 1682 (s, CHO), 1600 (s, $-C=C_{aryl}-$), 1219 (vs, $C_{phenyl}-OR$) cm^{-1}. UV−vis ($CHCl_3$, 1.3×10^{-5} M): λ_{max}/nm (ϵ/(L mol^{-1} cm^{-1})): 261 (46 230), 283.4 (48 420), 329.6 (26 190), 381.6 (14 570), 480.8 (57 400), 512.0 (71 140). Anal. Calcd for $C_{64}H_{80}O_6$ (945.33): C, 81.32; H, 8.53. Found: C, 81.31; H, 8.99.

Benzyldiethylphosphonate (**11**). A mixture of benzyl bromide (**10**) (10 g, 0.058 mol) and an excess of triethyl phosphite (19 g, 0.114 mol) was heated slowly to 150 °C, and the evolving ethyl bromide was distilled off simultaneously. After heating 4 h at 150 °C, vacuum was applied for 1 h to remove the excess of triethyl phosphite. Benzyldiethylphosphonate was obtained at 1.5 mbar and 120 °C as a colorless liquid. Yield: 11.5 g (87%). ^{1}H NMR (250 MHz, $CDCl_3$): δ/ppm = 1.19 (6H, t, ^3J = 7.05 Hz, CH_3-), 3.10 (2H, d, $^3J = 21.56$ Hz, CH_2P-), 3.99 (4H, q, $^3J = 6.45$ Hz, $-CH_2O-$), 7.17 → 7.30 ($C_{phenyl}-H$'s). ^{13}C NMR (62 MHz, $CDCl_3$): δ/ppm = 15.92, 16.23, 16.33 (CH_3-), 32.63, 34.83 ($-CH_2P-$), 61.95, 62.06 ($-CH_2O-$), 126.74, 126.80, 128.41, 128.46, 129.65, 129.76, 131.51, 131.65 (C_{phenyl}'s).

Poly{1,4-(2,5-dioctyloxyphenylene)ethynylene-1,4-[2,5-di(2-ethylhexyloxy)phenylene]-1,4-(2,5-dioctyloxyphenylene)-ethene-1,2-diyl-1,4-[2,5-di(2-ethylhexyloxy)phenylene]ethene-1,2-diyl} **(13cc)**. Dialdehyde **7c** (1 g, 0.906 mmol) and bisphosphonate **12c** (575.15 mg, 0.906 mmol) were dissolved in dried toluene (40 mL) while stirring vigorously under argon and heating under reflux. Potassium *tert*-butoxide (600 mg, 5.36 mmol) was added to this solution. After 2 h heating at reflux, three drops of benzyldiethylphosphonate (**11**) were added; 30 min later three drops of benzaldehyde were also added with an additional 100 mg of potassium *tert*-butoxide. After a total reaction time of 3 h, more toluene was added, and the reaction was quenched with aqueous HCl. The organic phase was separated and extracted several times with distilled water until the water phase became neutral (pH = 6−7). The organic layer was dried in a Dean−Stark apparatus. The resulting toluene solution was filtered and evaporated under vacuum to the minimum, and the polymer was precipitated in methanol. The polymer was extracted for 8 h with methanol, dissolved once more in toluene, reprecipitated in methanol, and dried under vacuum. Thus, 1.0 g (77.2%) of orange-red polymer was obtained. GPC (THF): $\bar{M}_n = 18\,000$ g/mol, $\bar{M}_w$ = 90 000 g/mol, $\bar{M}_z = 280\,000$ g/mol, $M_p = 49\,000$ g/mol; PDI = 5.0. ^{1}H NMR (400 MHz, $CDCl_3$): δ/ppm = 0.85 → 1.85 [120H, $-(CH_2)_6CH_3$ and $-CH(CH_2CH_3)(CH_2)_3CH_3$], 3.49 → 4.09 (16H, $-CH_2O-$), 6.81 → 7.16 (8H, phenylene H's), 7.43 → 7.50 (4H, vinylene H's). ^{13}C NMR (100 MHz, $CDCl_3$): δ/ppm = 11.64 (CH_3- ethyl), 14.40 (CH_3- hexyl and octyl), 23.03, 23.46, 24.47, 24.70, 26.47, 29.69, 31.06, 31.30, 32.23 ($-(CH_2)_3-$ hexyl and $-(CH_2)_6-$ octyl), 40.10, 40.23 (−CH−), 69.19, 69.90, 70.30, 72.30, 72.55 ($-CH_2O-$), 91.33, 92.27 ($-C\equiv C-$), 110.67, 111.13, 113.64, 114.87, 117.51, 117.82, 119.02 ($C_{phenyl}-H$), 123.26, 124.65 (vinylene C's), 127.38, 127.93, 129.26 ($C_{phenyl}-C$), 150.93, 151.74, 154.20, 154.55 ($C_{phenyl}-OR$). IR (FTIR): 3055 (vw, $C_{aryl}-H$), 2956, 2923, and 2856 (s, $-CH_3$ and $-CH_2-$), 2201 (vw, disubst $-C\equiv C-$), 1599 (w, $-C=C_{phenyl}-$), 1251 and 1199 (vs, $C_{aryl}-OR$), 970 cm^{-1} (trans $-CH=CH-$). UV−vis ($CHCl_3$, 8.8×10^{-6} M): λ_{max}/nm (ϵ/(L mol^{-1} cm^{-1})) 318 (29 600), 470 (105 200). Anal. Calcd for $(C_{96}H_{148}O_8)_n$ $(1430.22)_n$: C, 80.62; H, 10.43. Found: C, 80.24; H, 10.37.

Poly[1,4-(2,5-dioctyloxyphenylene)ethynylene-1,4-(2,5-dioctyloxyphenylene)-1,4-(2,5-dioctyloxyphenylene)ethene-1,2-diyl-1,4-(2,5-dioctyloxyphenylene)ethene-1,2-diyl] **(13bb).** Dialdehyde **7b** (1.655 g, 1.5 mmol) and bisphosphonate **12b** (953 mg, 1.5 mmol) were dissolved in dried toluene (40 mL) while stirring vigorously under argon and heating under reflux. Potassium *tert*-butoxide (994 mg, 8.87 mmol) was added to this solution. After 1 h heating at reflux, 0.6 g of benzyldiethylphosphonate (**11**) was added; 30 min later 0.6 g of benzaldehyde was also added with additional 100 mg of potassium *tert*-butoxide. After a total reaction time of 3.5 h, more toluene was added, and the reaction was quenched with aqueous HCl. The organic phase was separated and extracted several times with distilled water until the water phase became neutral (pH = 6−7). The organic layer was dried in a Dean−Stark apparatus. The resulting toluene solution was filtered and evaporated

Scheme 1

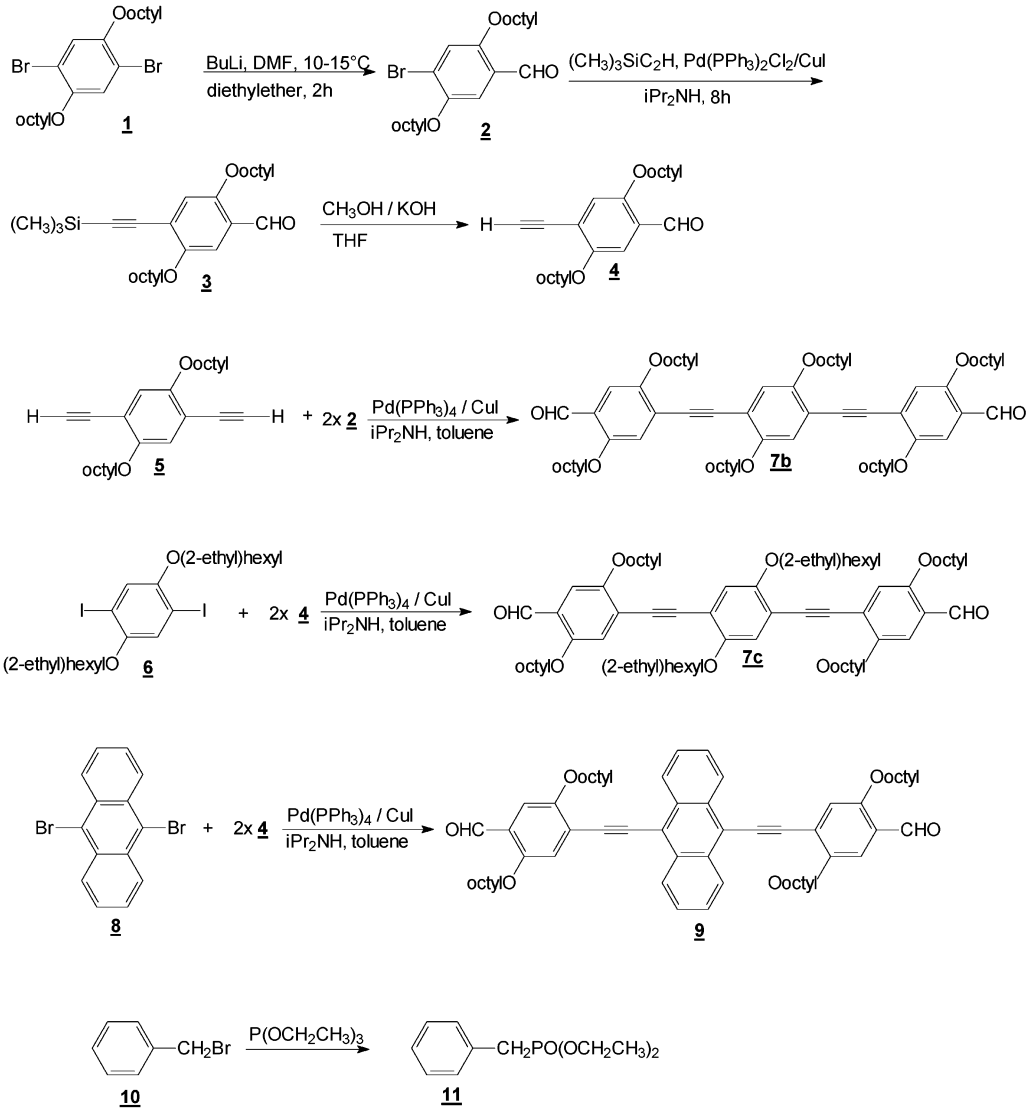

under vacuum to the minimum (60 mL), and the polymer was precipitated in methanol (400 mL). The polymer was extracted for 8 h with methanol and dried under vacuum. Thus, 1.9 g (88%) of orange-red polymer was obtained. GPC (THF): $\bar{M}_n$ = 16 300 g/mol, $\bar{M}_w$ = 37 100 g/mol, $\bar{M}_z$ = 67 300 g/mol, M_p = 35 700 g/mol; PDI = 2.27. ^{1}H NMR (400 MHz, $CDCl_3$): δ/ppm = 0.85−0.87 (24H, CH_3−), 1.27−1.86 (96H, −$(CH_2)_6$−), 3.62−3.66 and 3.90−4.10 (16H, −CH_2O−), 6.72−7.14 (C_{phenyl}−H), 7.43−7.48 (−CH=CH−). ^{13}C NMR (100 MHz, $CDCl_3$): δ/ppm = 14.45 (CH_3−), 23.06, 26.46, 26.50, 26.65, 29.74, 29.85, 32.28 (−(CH_2)−), 69.15, 69.83, 69.95, 70.23, 70.42 (−CH_2O−), 91.24, 92.41 (−C≡C−), 111.20, 111.53, 114.94, 117.24, 117.69, 117.88 (C_{phenyl}−H), 123.73, 124.92 (−CH=CH−), 113.50, 119.06, 126.38, 127.94, 129.22 (C_{phenyl}−C), 151.00, 151.62, 153.96, 154.52 (C_{phenyl}−OR). IR (KBr): 3059 (vw, C_{phenyl}−H), 2924 and 2853 (vs, −CH_2− and CH_3−), 2203 (vw, disubst −C≡C−), 1747 (vw, −CHO), 1600 (−C=C_{phenyl}−), 1206 (C_{phenyl}−OR), 968 cm^{-1} (m, *trans*-CH=CH−). UV−vis ($CHCl_3$, 6.57 × 10^{-6} M): λ_{max}/nm (ϵ/(L mol^{-1} cm^{-1})): 320.8 (24 000), 469 (69 300). Anal. Calcd for $(C_{96}H_{148}O_8)_n$ (1430.22)$_n$: C, 80.62; H, 10.43. Found: C, 79.82; H, 10.28.

Poly[1,4-(2,5-dioctyloxyphenylene)ethynylene-8,9-anthracenyleneethynylene-1,4-(2,5-dioctyloxyphenylene)ethene-1,2-diyl-1,4-(2,5-dioctyloxyphenylene)ethene-1,2-diyl] (**14**). Dialdehyde **9** (501 mg, 0.53 mmol) and bisphosphonate **12a** (485 mg, 0.53 mmol) were dissolved in dried toluene (50 mL) while stirring vigorously under argon and heating under reflux. Potassium *tert*-butoxide (238 mg, 2.12 mmol) was added to this solution; the reaction mixture was heated at reflux for 3 h. After this time more toluene was added, and the reaction was quenched with aqueous HCl. The organic phase was separated and extracted several times with distilled water until the water phase became neutral (pH = 6−7). The organic layer was dried in a Dean−Stark apparatus. The resulting toluene solution was filtered, evaporated under vacuum to the minimum, and precipitated in methanol. The polymer was extracted with methanol/water for 10 h, dissolved once more in toluene, reprecipitated in methanol, and dried under vacuum. 715 mg (86.8%) of purple-red polymer was obtained.

GPC (THF): $\bar{M}_w$ = 51 190 g/mol, $\bar{M}_n$ = 25 570 g/mol, $\bar{M}_z$ = 144 400 g/mol, M_p = 44 700 g/mol, PDI = 2.0. ^{1}H NMR (400 MHz, $CDCl_3$): δ/ppm = 0.84−2.05 (130H, m,$CH_3(CH_2)_{16}$− and $CH_3(CH_2)_6$−), 3.62 → 4.20 (12H, m, −CH_2O−), 6.84−6.91; 7.19; 7.51−7.60 and 8.84 (18H, −arylene and vinylene H's). ^{13}C NMR (100 MHz, $CDCl_3$): δ/ppm = 14.07, 22.66, 26.22, 29.29, 29.34, 29.47, 29.53, 29.70, 31.87, 31.89 ($CH_3(CH_2)_{16}$− and $CH_3(CH_2)_6$−), 69.35, 69.55, 69.71 (−CH_2O−), 116.95, 126.47, 127.59, 132. 07, 150. 54, 154.56 (arylene and vinylene C's). IR (KBr): 3057 (w, C_{phenyl}−H), 2923 and 2852 (vs, CH_3 and −CH_2−), 2184 (vw, −C≡C−), 1597 (w, −C=C_{aryl}−), 1203 (s, C_{phenyl}−OR), 971 cm^{-1} (m, trans −CH=CH−). UV−vis ($CHCl_3$, 9.1 × 10^{-6} M): λ_{max}/nm (ϵ/(L mol^{-1} cm^{-1})): 284 (42 500), 328 (19 000), 408.8 (18 500), 547.2 (82 200), 587.2 (32 500). Anal. Calcd for $(C_{108}H_{160}O_6)_n$ (1554.45)$_n$: C, 83.44; H, 10.37. Found: C, 80.29; H, 10.53.

Scheme 2

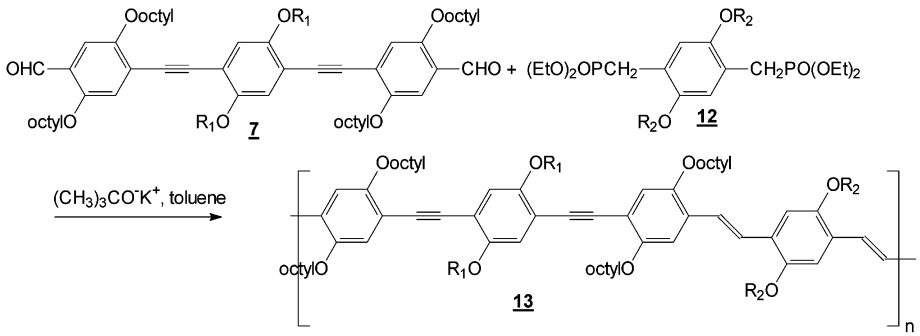

7a, **12a**: $R_1 = R_2$ = octadecyl.
7b, **12b**: $R_1 = R_2$ = octyl.
7c, **12c**: $R_1 = R_2$ = (2-ethy)lhexyl .

13aa: $R_1 = R_2$ = octadecyl.
13ab: R_1 = octadecyl, R_2 = octyl.
13bb: $R_1 = R_2$ = octyl.
13cc: $R_1 = R_2$ = (2-ethyl)hexyl.

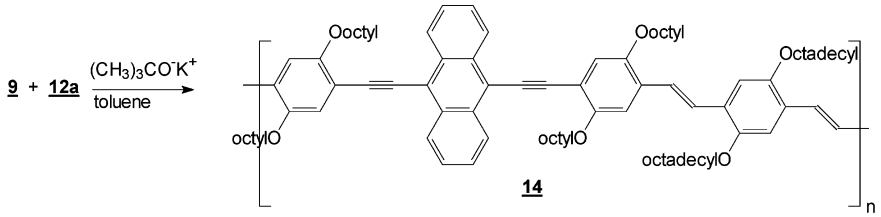

Results and Discussion

The syntheses of the various 2,5-dialkoxy-*p*-xylylene-bis(diethylphosphonate)s (**12a**−**c**) and of the fluorophoric dialdehyde **7a** [1,4-bis(formyl-2,5-dioctyloxyphenylethynyl)-2,5-dioctadecyloxybenzene] have been reported elsewhere.[14] Scheme 1 depicts the various synthetic steps leading to dialdehydes **7b**, **7c**, and **9**. The Bouveault formylation[22] of 1,4-dibromo-2,5-dioctyloxybenzene (**1**) and subsequent chromatographic purification provided 1-formyl-4-bromo-2,5-dioctyloxybenzene (**2**) in 74.6% yield alongside negligible among of 2,5-dioctyloxyterephthalaldehyde. The Pd-catalyzed ethynylation of **2** with trimethysilylacetylene afforded 2,5-dioctyloxy-4-trimethylsilylbenzaldehyde (**3**) in 84% yield, whose hydrolysis with KOH/MeOH led to 4-ethynyl-2,5-dioctyloxybenzaldehyde in 65% yield. The Pd-catalyzed cross-coupling reactions[4,23] of 1,4-diethynyl-2,5-dioctylbenzene[19] (**5**) with 2 equiv of **2** and of 1,4-diiodo-2,5-bis(2-ethylhexyloxy)benzene[14c,20] with 2 equiv of **4** led to dialdehyde **7b** [1,4-bis(formyl-2,5-dioctyloxyphenylethynyl)-2,5-dioctyloxybenzene] in 69% yield and **7c** [1,4-bis(formyl-2,5-dioctyloxyphenylethynyl)-2,5-di(2-ethyl)hexyloxybenzene] in 55% yield, respectively. A small amount (6.8%) of 1,4-bis[(4-formyl-2,5-dioctyloxy)-phenyl)]but-1,3-diyne (**15**) was obtained alongside **7c**. The dialdehyde **9** (9,10-bis[(4-formyl-2,5-dioctyloxy)-phenylethynyl]anthracene) was synthesized through the cross-coupling reaction of 9,10-dibromoanthracence[21] with 2 equiv of **4**; it was obtained as a purple-red substance in a yield of 60.5% after purification through column chromatography. All the peaks from the ^{13}C NMR spectra of **7c** and **9** in deuterated chloroform can be readily assigned to their corresponding carbons.

Polymers **13** and **14** were obtained through the Horner−Wadsworth−Emmons olefination reaction[24] of dialdehydes **7** or **9** with bisphosphonates **12** as depicted in Scheme 2. End-capping was carried out in the case of **13bb** and **13cc** by adding freshly distilled benzaldehyde and benzyldiethylphosphonate (**11**) (obtained from the Michealis−Arbuzov reaction of benzyl bromide (**10**) and triethyl phosphite in 87% as shown in Scheme 1) in the reaction medium after a reaction time of 2 h. The polymers were obtained in yields above 70% as orange-red materials in the case of **13** and as a dark purple-red substance in the case of **14**. All the polymers were readily dissolved in common organic solvents such as THF, chloroform, toluene, chlorobenzene, and dichloromethane. The chemical structures of the polymers were confirmed by IR (KBr), ^1H NMR, ^{13}C NMR, and elemental analysis. The ^{13}C NMR (100 MHz, $CDCl_3$) of polymer **13cc** is similar to that of **13ab**,[14c] apart from the additional signals at 11 and 40 ppm typical of 2-ethylhexyloxy side groups. From the ^1H NMR (400 MHz, $CDCl_3$) of **14**, the protons of the alkyl side chains appear upfield in the region between 0.84 and 2.05 ppm. The signals of the protons of the $-CH_2-$ group adjacent to oxygen were detected between 3.62 and 4.20 ppm. The vinylene and arylene protons peaks were found downfield between 6.84 and 8.84 ppm. The average molecular weights were measured by gel permeation chromatography (GPC) with polystryrene as standards. THF served as the eluting solvent. The number-average-molecular weights, $\bar{M}_n$, were between 15 000 and 30 000 g/mol, leading to degrees of polymerization (DP) between 11 and 17. The polydispersity indexes (PDI) were found between 2 and 3 except for **13cc**, whose PDI was 5. Data from GPC are given in Table 1.

Table 1. Data from GPC (TFH) with Polystyrene as Standard and Thermal Stabilities[a]

code	$\bar{M}_n$	$\bar{M}_w$	M_p	PDI	$\bar{D}P$	$T_{5\%}$/°C	$T_{10\%}$/°C
13ab	29 400	82 500	66 500	2.8	17	386	424
13aa	27 500	62 400	53 300	2.2	14	361	400
13bb	16 300	37 100	35 500	2.2	12	356	381
13cc	15 400	77 200	51 000	5.0	11	352	379
14	25 600	51 200	44 700	2.0	16	350	371

[a] Values are given for 5%, $T_{5\%}$, and 10%, $T_{10\%}$, weight loss.

According to thermogravimetric analysis (TGA), the polymers are thermostable compounds. The start of the

Table 2. Data from the UV−Vis Absorption Spectroscopy in Dilute Chloroform Solution and in the Solid State (Thin Films of 100−150 nm Thickness Spin-Casted from Chlorobenzene Solution)

code	concn/M	$\lambda_{max,abs}$/nm	ϵ_{max}/M^{-1} cm^{-1}	$\lambda_{10\%max}$/nm	λ_T/nm	$E_g^{opt}{}_{(10\%)}$/eV[a]	$E_g^{opt}{}_{(T)}$/eV[b]
7a	0.93×10^{-5}	421	60 750	478	465	2.59	2.66
7b	1.85×10^{-5}	423	57 060	474	468	2.61	2.64
7c	1.10×10^{-5}	423	51 300	472	468	2.62	2.64
9	1.30×10^{-5}	512	71 140	534	534	2.32	2.32
13ab	8.6×10^{-6} [c]	472	101 160[c]	520	522	2.38	2.37
13ab[d]	7.6×10^{-3} [c]	491		551	554	2.25	2.24
13aa	6.2×10^{-6} [c]	468	86 300[c]	521	520	2.38	2.38
13aa[d]	5.0×10^{-3} [c]	496		558	560	2.22	2.21
13bb	7.0×10^{-6} [c]	469	69 310[c]	524	523	2.36	2.37
13bb[d]	1.4×10^{-2} [c]	484		554	557	2.24	2.23
13cc	8.8×10^{-6} [c]	470	105 200[c]	521	523	2.38	2.37
13cc[d]	1.4×10^{-2} [c]	485		551	554	2.25	2.24
14	9.1×10^{-6} [c]	*547* (sh: 587)	82 240[c]	614	622	2.01	1.99
14[d]	1.3×10^{-2} [c]	548, *581*		651	633	1.90	1.95

[a] $E_g^{opt}{}_{(10\%)} = hc/\lambda_{10\%max}$. [b] $E_g^{opt}{}_{(T)} = hc/\lambda_T$. [c] Per mole of the constitutional unit. [d] Solid state.

Table 3. Photoluminescence Data in Dilute Chloroform Solution (~10^{-8} M) and in Solid State[a]

code	λ_{exc}/nm	$\lambda_{max,em}$/nm	Stokes shift/nm	fwhm/nm	ϕ_{fl}/%
7a	423	466	43	53	73
7b	424	468	45	53	65
7c	424	468	45	58	67
9	512	524 (sh: 563)	12	26	80
13ab	472	519 (sh: 560)	47	36	70
13ab[a]	491	*553*, 591	62	114	29
13aa	472	519 (sh: 560)	47	37	77
13aa[a]	496	*552*, 592	56	67	54
13bb	464	520 (sh: 560)	51	67	60
13bb[a]	484	559, *593*	109	119	23
13cc	472	521(sh: 560)	51	59	65
13cc[a]	485	*542*, 582	57	67	45
14	515	577 (sh: 615)	30	45	56
14[a]	581	622 (sh: 665)	41	78	24

thermal degradation under air lies between 350 and 386 °C, where 5% weight loss was recorded (Table 1). No glass transition temperature, T_g, was obtained for all polymers by DSC measurements while heating to 295 °C.

The photophysical characteristics of polymers **13** and **14** and the monomers **7** and **9** were studied by UV−vis absorption and photoluminescence in dilute chloroform solution (concentration ≈ 10^{-6} M) as well as in the solid state. The absorption maxima, $\lambda_{max,abs}$, the solution concentrations, the extinction coefficients at the maximum wavelength, ϵ_{max}, and the optical band gap energies, E_g^{opt}, are given in Table 2. Two ways to determine the E_g^{opt} of each substance have been presented in Table 2, namely from values of 10% of the absorption maximum (taken from the lower energy side), $\lambda_{10\%max}$, and of the intersection of the tangential through the turning point of the lower energy side of the spectrum and the lengthened baseline for each substance, λ_T.[25] Both determination methods lead to identical results only when the slope of lower energy side is steep enough, which is also a prerequisite for the determination of the E_g^{opt} from the cross-point between absorption and emission spectra.[15d] This condition is fulfilled by all our compounds except **14**, whose solution absorption spectrum has a lower energy shoulder at 587 nm. The excitation wavelengths, λ_{exc}, the emission maxima, $\lambda_{max,em}$, the Stokes shift, the full width at half-maximum (fwhm) of the emission curves, and the fluorescence quantum yields, ϕ_{fl}, are presented in Table 3. All the emission data given here were obtained after exciting at the main absorption peak.

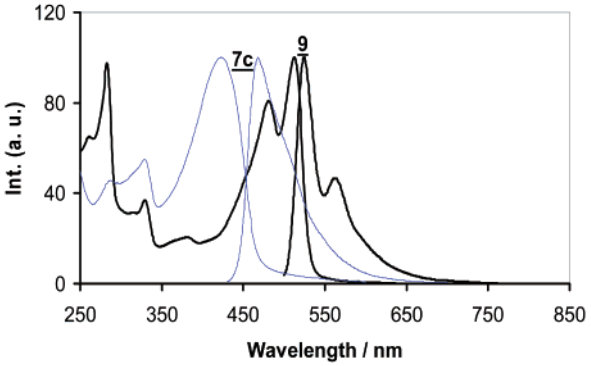

Figure 1. Absorption and emission spectra in dilute $CHCl_3$ solution of monomers **7c** and **9**.

Figure 1 illustrates the absorption and emission spectra of monomer **7c** (representative of all the monomers of type **7**) and of the anthracene-containing monomer **9**. Monomers **7** are characterized with absorption maxima at 421−423 nm and emission maxima around 468 nm. An optical band gap energy of 2.60 eV, extinction coefficients around 60 000 M^{-1} cm^{-1}, and quantum yields between 60 and 70% were obtained for these compounds. The presence of anthracenylene unit in **9** leads to a 90 nm bathochromic shift of its $\lambda_{max,\ abs}$ located at 512 nm (E_g^{opt} = 2.3 eV, ϵ = 71 140 M^{-1} cm^{-1}), relative to **7**. Its well-resolved fluorescence curve has its maximum at 524 nm and a low-energy peak at 563 nm. The very sharp emission of **9** is characterized with a fwhm value of 26 nm and a Stokes shift of 12 nm, which are less than half of the corresponding values of **7**, resulting in a higher fluorescence quantum yield of 80% after exciting at 512 nm or ϕ_{fl} > 95%, when the excitation was done at 480 nm.

Identical absorption spectra were obtained for all polymers **13** in dilute chloroform solution, which are characterized with a maximum peak around 470 nm (Figure 2). As expected is the anthracene-containing polymer **14** red-shifted relative to **13**; its absorption spectrum consists of a maximum at 547 nm and a shoulder at 587 nm. Optical band gap energies of 2.36−2.38 and 2.0 eV are obtained for **13** and **14**, respectively; their extinction coefficients are between 70 000 and 100 000 M^{-1} cm^{-1}. The dilute solution emission spectra of polymers **13** are well-resolved and are made up of a maximum at 520 nm and a low-energy shoulder at 560 nm. However, both the intensity of the shoulder relative to the main peak and the fwhm value increase from the *long linear* (octadecyloxy) side chains polymers (fwhm

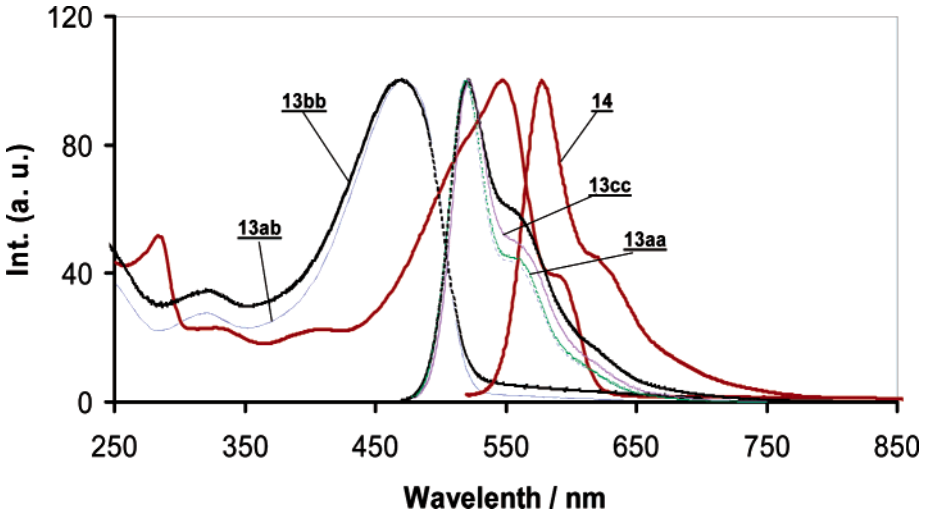

Figure 2. Absorption and emission spectra in dilute $CHCl_3$ solution of polymers **13** and **14**.

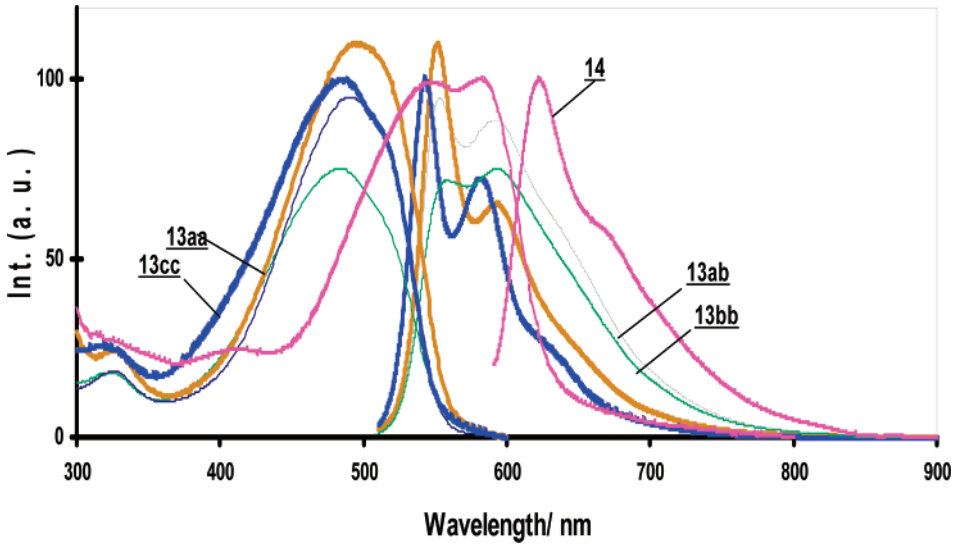

Figure 3. Solid-state absorption and emission spectra of polymers **13** and **14** (thin films spin-casted from 10^{-2} to 10^{-3} M chlorobenzene solution).

= 36 nm for both **13aa** and **13ab**) over the *short branched* (2-ethylhexyloxy) side chains polymer (fwhm = 51 nm for **13cc**) to the *short linear* side chains polymer (fwhm = 67 nm for **13bb**). From these observations, one can ascribe the emission from the long side chains polymers as coming basically from isolated main chain fluorophores; the emission from short side chains polymers is a contribution of isolated main chain fluorophores and a certain degree of aggregation. This can be attributed to the lyotropic behavior of this class of compounds as observed on polarized optical microscopy.[14b,c] The ϕ_{fl} values between 60% and 80% were obtained for these compounds. The shape of the emission curve of **14** is similar to that of **13**; it is however red-shifted and consists of a maximum at 577 nm and a shoulder at 615 nm. Its fwhm value of 45 nm is closer to those of **13aa** and **13ab**, due to the presence of octadecyl side chains. The existence of a strong overlap of the absorption and emission spectra, greatly inducing self-reabsorption might explain the relatively (to **13**) lower photoluminescence quantum yield of 56% for **14**, despite its lower Stokes shift of 30 nm.

The properties of conjugated polymers thin films are quite sensitive to chain packing morphology, which can vary dramatically depending on preparation conditions.[1d] Transparent thin films of our polymers were spin-casted on a quartz substrate from a chlorobenzene solution (concentration ≈ 10^{-3}−10^{-2} M), leading to thicknesses between 100 and 150 nm. Chlorobenzene as solvent is known to interact preferentially with aromatic rings, causing the polymer chains to lie open and flat and thereby enhancing π-stacking between neighboring chains and aggregate formation.[26] This contributes to lower the photoluminescence efficiency of the polymers in thin films compared to the solution. The enhanced planarization of the conjugated backbone gives rise to the bathochromic shift of the absorption and emission spectra of the polymers **13** and **14** in the solid state, shown in Figure 3, as compared to their solution samples.

Contrary to the solutions where the dependence of the photophysical properties of polymers **13** on the side groups is minimal, the solid-state properties are greatly dependent on the *nature* (linear or branched), *size*, and *location* of the grafted alkoxy side groups. The absorption maximum of polymers **13aa**, **13ab**, **13bb**, and **13cc** appears at 496, 491, 484, and 485 nm, respectively, clearly indicating that longer side groups (R_1 and/or R_2 = octadecyl) enable a bathochromic shift of the maximum peak. An optical band gap energy, E_g^{opt}, of 2.21−

2.24 eV was obtained for these compounds. The anthracene-containing compound **14** has a red-shifted absorption curve, which consists of two maxima at 548 and 581 nm (corresponding respectively to the solution main peak at 547 nm and the shoulder peak at 587 nm) and an E_g^{opt} of 1.90 eV.

The grafting of longer linear side chains (octadecyl in **13aa**) or short branched side chains (2-ethylhexyl in **13cc**) at position R_2 provides very sharp and well-resolved emission spectra. An identical fwhm value of 67 nm was obtained for both polymers; however, the positions of their maxima are different. While the emission peaks in **13aa** are found at 552 and 592 nm, those in **13cc** are 10 nm blue-shifted and are located at 542 and 582 nm, which may be due to a greater nonplanarity of the conjugated backbone resulting from the presence of the bulky branched 2-ethylhexyl side chains. The curve of **13cc** moreover shows a tailed emission in the region of 600−670 nm. The intensity of the peak at 552 nm for **13aa** or at 542 nm for **13cc** is greatly higher than that at 592 nm for **13aa** or at 582 nm for **13cc**. The shape of their emission curves and their high fluorescence quantum yields of 54% (**13aa**) and 45% (**13cc**) are evidence of minimal contribution of aggregation species (excimers) during the photoluminescence process.

Excimer contributions are clearly evident in the case of polymers **13ab** and **13bb** having short linear side chains (R_2 = octyl) at the phenylene−vinylene segments, which are reflected by the shape of their curves, their relatively (to **13aa** and **13cc**) higher fwhm values of 114 nm (for **13ab**) and 119 nm (for **13bb**), and lower fluorescence quantum yields of 29% (for **13ab**) and 23% (for **13bb**). Although the grafting of longer side chains (octadecyl) at R_1 in **13ab** does not lead to the same effect as when grafted at R_2, it however contributes, to a smaller extent, in the limitation of the excimer emission. This explains the differences in emission data (fwhm values, Stokes shift and ϕ_{fl}) obtained for **13ab** and **13bb**, which has both R_1 and R_2 equal to octyl. While in **13ab** the emission peak at 553 nm is more intense than that at 591 nm, in **13bb** the maximum at 553 nm is slightly lower than that at 592 nm.

The emission spectrum of the film of **14** is of almost similar shape as the solution sample, although red-shifted. It consists of a maximum at 621 nm and a shoulder at 665 nm. A fwhm value of 78 nm and a photoluminescence quantum yield of 24% were obtained for this compound.

Both types of polymers **13** and **14** are photoconductive even without any sensitizer (Figure 4). Three thin film samples of each polymer, obtained from chlorobenzene solution, and of thickness between 100 and 150 nm, were measured for the purpose of reproducibility. Photoconductivity is detected already at 10 V from polymers **13aa**, **13ab**, and **14**, which have in common octadecyloxy side groups, confirming the assumption that photoconductivity is more an intramolecular process than an intermolecular one.[14c] The maximum photocurrent, I_{ph}, was 1.1×10^{-9} A at 20 000 cm^{-1} for **13aa**, 3.9×10^{-11} A at 18 900 cm^{-1} for **13ab**, and 3.8×10^{-11} A at 16 800 cm^{-1} for **14**. A voltage of 20 V is needed to detect photoconductivity from polymers with shorter side groups, **13bb** and **13cc**. I_{ph} of **13bb** was 2.0×10^{-10} A at 20 000 cm^{-1}. The photoconductivity spectra of all polymers were approximately reproducible except **13cc**, whose three measured samples provided spectra having

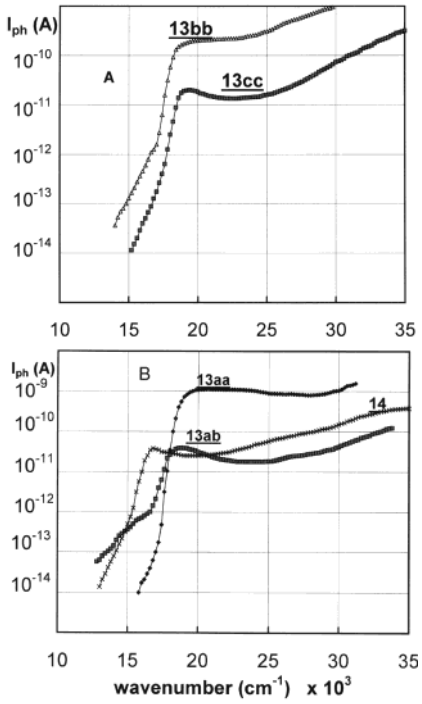

Figure 4. Photoconductivity spectra of thin films of polymers **13** and **14** [surface type cell, slit width 0.2 mm, light intensity 20 μW, threshold voltage of 20 V (A) and of 10 V (B)].

maximum photocurrents ranging from 2.0×10^{-11} A at 19 400 cm^{-1} to 2.0×10^{-10} A at 19 000 cm^{-1}, probably as a result of different conformational structures caused by the bulky 2-ethylhexyl side chains.

When materials are used as an emissive layer for organic light-emitting diodes (OLEDs) or as a donor (or acceptor) component in organic photovoltaic devices (OPVDs), matches of their valence band (HOMO) and their conduction band (LUMO) energy levels with work functions of the electrodes and/or with the HOMO and LUMO energy levels of other components of the OPVDs as well as their optical, electrical, and chemical stability are of paramount importance. The ionization potential (IP, i.e., the highest occupied molecular orbitals (HOMO) of an organic molecule) is determined through ultraviolet photoelectron spectroscopy.[27] The electron affinity (EA, i.e., the lowest unoccupied molecular orbitals (LUMO) of the organic molecule) is deduced from the IP value and the band gap obtained from the absorption spectrum, which is not a direct means of determination. Cyclic voltammetry (CV) and/or differential pulse polarography (DPP) are easy and effective methods to measure redox potentials and to simultaneously evaluate both the HOMO and LUMO energy levels and the band gap energy, E_g^{ec}, of a polymer. The electrochemical processes are similar to the charge injection and transport in LED and photovoltaic devices.

The CV was carried out in dichloromethane at a potential scan rate of 167 mV/s and the DPP at 20 mV/s. Ag/AgCl served as the reference electrode; it was calibrated with ferrocene ($E^{1/2}_{ferrocene}$ = 450 mV vs Ag/AgCl). The working and the counter electrodes were a platinum disk. The supporting electrolyte was tetrabutylammonium hexafluorophosphate (n-Bu_4NPF_6) in anhydrous dichloromethane (10^{-3} M). The onset potentials are the values obtained from the intersection of the two tangents drawn at the rising current and the baseline charging current of the CV and the DPP curves.

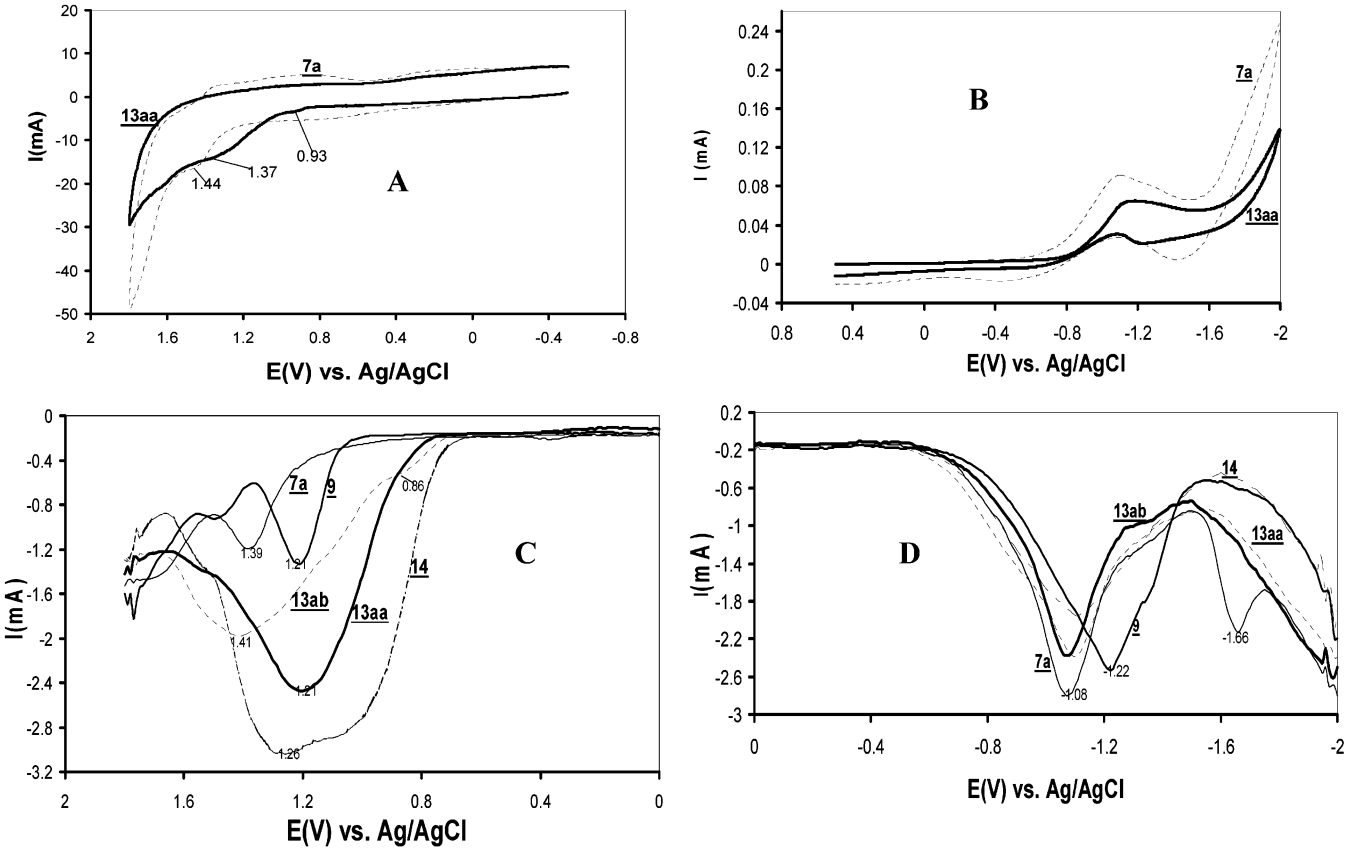

Figure 5. Cyclic voltammetry for oxidation (A) and reduction (B) of monomer **7a** and polymer **13aa** and differential pulse polarography for oxidation (C) and reduction (D) of monomers **7a** and **9** and polymers **13aa**, **13ab**, and **14**.

Table 4. Redox Potentials (vs Ag/AgCl), Electrochemical Energy Gaps, HOMO and LUMO Energies As Obtained from Cyclic Voltammetry and Differential Pulse Polarography[c]

code	$E^{red/onset}$/V	$E^{red/peak}$/V	$E^{ox/onset}$/V	$E^{ox/peak}$/V	$E_g^{ec/onset}$/eV	$E_g^{ec/peak}$/eV	E^{HOMO}/eV	E^{LUMO}/eV
7a[a]	−0.73	−1.09	1.32	1.43	2.05	2.52	−5.67	−3.62
7a[b]	−0.76	−1.08	1.28	1.39	2.04	2.46	−5.63	−3.59
9[a]	−0.85	−1.18	1.16	1.28	2.01	2.46	−5.51	−3.50
9[b]	−0.80	−1.22	1.10	1.21	1.90	2.43	−5.45	−3.55
13ab[a]	−0.80	−1.10	0.80	0.85	1.60	1.95	−5.15	−3.55
13ab[b]	−0.70	−1.07	0.77	1.41	1.47	2.48	−5.12	−3.65
13aa[a]	−0.88	−1.19	0.88	0.93	1.76	2.12	−5.23	−3.47
13aa[b]	−0.65	−1.10	0.87	1.21	1.52	2.31	−5.22	−3.70
13bb[a]	−0.75	−1.09	0.80	0.88	1.55	1.97	−5.15	−3.60
13bb[b]	−0.60	−0.97	0.77	1.43	1.37	2.40	−5.12	−3.75
13cc[a]	−0.76	−1.21	0.88	0.93	1.64	2.14	−5.23	−3.59
13cc[b]	−0.76	−1.12	0.80		1.56		−5.15	−3.59
14[a]	−0.84	−1.24	0.71	0.90	1.54	2.14	−5.06	−3.51
14[b]	−0.67	−1.10	0.75	1.26	1.42	2.38	−5.10	- 3.68

[a] Obtained from cyclic voltammetry. [b] Obtained from differential pulse polarography. [c] $E^{HOMO}/E^{LUMO} = [-(E^{onset} - 0.45) - 4.8]$ eV where the value 0.45 V for ferrocene vs Ag/Ag^+ and 4.8 eV the energy level of ferrocene below the vacuum.

Several ways to evaluate HOMO and LUMO energy levels from the onset potentials, $E^{ox/onset}$ and $E^{red/onset}$, have been proposed in the literature.[25,28−31] They were estimated here on the basis of the reference energy level of ferrocene (4.8 eV below the vacuum level)[29] according to the following equation: $E^{HOMO}/E^{LUMO} = [-(E^{onset} - 0.45) - 4.8]$ eV. Figure 5 shows representatively the CV traces for oxidation and reduction of **7a** and **13aa** the DPP traces for oxidation and reduction of **7a**, **9**, **13aa**, **13ab**, and **14**. The onset and the peak potentials, the electrochemical band gap energy, and the estimated position of the upper edge of the valence band (HOMO) and of the lower edge of conduction band (LUMO) are listed in Table 4.

The CV for oxidation did not provide clear and sharp peaks. Peaks of very low intensity were obtained around 0.90 V with estimated onset values around 0.80 V obtained for all polymers. **13aa**, moreover, shows a very shallow second oxidation peak around 1.37 V. The oxidation CV traces of the monomers **7** and **9** show peaks respectively at 1.44 V (onset at 1.32 V) and 1.28 V (onset at 1.16 V). The CV reduction process was reversible for all compounds. Reduction peaks around −1.10 to −1.20 V (onset values between −0.70 and −0.88 V) were obtained. These values were confirmed by the DPP reduction processes ($E^{red/peak} = -0.97$ to −1.22 V and $E^{red/onset} = -0.65$ to −0.80 V). In comparison with the reduction, the DPP oxidation processes provided broader signals for the polymers than for the monomers. The curve of the electron-rich anthracene-containing polymer **14** has the smallest onset value of 0.75 V and a very broad almost plateaulike maximum,

whose lowest point was located at 1.26 V. Its corresponding monomer **9** has its peak centered at 1.21 V with a relatively higher onset value of 1.10 V. 1.21 V is also the maximum of the oxidation peak of **13aa**, whose onset value at 0.87 V is smaller than that of its corresponding monomer **7a**, found at 1.28 V. The DPP peak of **7a** is found at 1.39 V. It is similar to that from its CV trace and is of almost the same range as those from the DPP oxidation curves of **13bb** (1.43 V) and **13ab** (1.41 V). Polymer **13ab** is moreover characterized with a shoulder peak at 0.86 V, which corresponds to the CV oxidation peak around 0.90 V of these polymers.

We assume from these observations that the broad DPP oxidation peak of the polymers is actually a superimposition of two oxidation steps. The first oxidation step occurs around the phenylene−vinylene segment of the polymer which can be linked to the shoulder peak at 0.86 V in the case of **13ab** or the very weak CV oxidation peaks around 0.90 V for all the polymers. These values are closer to 0.70 V of the oxidation peak potential of MEH−PPV measured under the same conditions.[32] The second oxidation step, which can be ascribed to the peaks around 1.40 V, involves the arylene−ethynylene part of the polymer.[33] The reduction peak potential at around −1.10 V proves that the reduction processes are limited basically on the arylene ethynylene section of the compounds due to the high electron affinity of the triple bonds.[23d] Despite the extended π-conjugation of the backbone of **13** and **14**, one can consider, to a certain extent, these compounds to be donor−acceptor copolymers. The phenylene−vinylene segment would act as the donor and the arylene−ethynylene segment as the acceptor. This would explain the great discrepancy between the band gap energy directly measured from CV and DPP ($E_g^{ec/onset} \approx 1.54$ eV) and the optical band gap energy. Similar differences between E_g^{opt} and E_g^{ec} were found in donor−acceptor poly(aryl ether)s by Chen et al.[34] The DPP oxidation and reduction peaks difference ($E_g^{ec/peak}$) is in the cases of **13aa** (2.31 eV), **13ab** (2.48 eV), and **13bb** (2.40 eV) almost identical to the optical band gap, $E_g^{opt} = 2.38$ eV, obtained from the solution absorption spectra. From the onset potentials, HOMO and LUMO energy levels were estimated around −5.10 to −5.20 eV and −3.50 to −3.70 eV, respectively.

Conclusion

Defect-free, thermostable, soluble, and transparent film-forming hybrid arylene−ethynylene/arylene−vinylene polymers **13** and **14** have been synthesized using the Horner−Wadsworth−Emmons olefination reactions between luminophoric dialdehydes **7** and **9** and bisphosphonate **12** and characterized through NMR, IR, and elemental analysis. Although similar absorption and emission spectra were obtained in dilute chloroform solution for all polymers **13**, the full width at half-maximum (fwhm) values and the relation between the intensity of main peak at 520 nm and the shoulder around 560 nm depend on the length of the attached side chains. The absorption and emission spectra of **14** ($E_g^{opt} = 1.90$ eV) are bathochromically shifted relative to **13** ($E_g^{opt} = 2.22-2.25$ eV) due to the presence of anthracenylene units in its backbone. The solid-state photophysical properties of **13** and **14** (photoconductivity, absorption, emission, fluorescence quantum yield, Stokes shift, and fwhm) greatly depend on the *nature* (linear or branched), *length*, and *location* of the grafted alkoxy side groups. Photoconductivity is easily detected in polymers having octadecyloxy chains (**13aa**, **13ab**, and **14**). Long linear (octadecyl) or short branched (2-ethylhexyl) side chains at position R_2 (in the phenylene−vinylene segment) are required to obtain sharp and well-resolved emission spectra accompanied by high fluorescence quantum yields. The quasi-donor (phenylene−vinylene segment) and -acceptor (arylene−ethynylene segment) nature of these polymers could explain the great discrepancy between the electrochemical band gap and optical band gap energies. These polymers are presently used in the design of OLEDS and organic photovoltaic devices.

Acknowledgment. We gratefully thank Dr. Eckhard Birckner for carrying out the photoluminescence measurements in solution.

Supporting Information Available: ^{13}C NMR spectrum (62 MHz, $CDCl_3$) of monomer **7c**, ^{13}C NMR spectrum (62 MHz, $CDCl_3$) of monomer **9**, ^{13}C NMR spectrum (100 MHz, $CDCl_3$) of polymer **13cc**, ^1H NMR spectrum (400 MHz, $CDCl_3$) of polymer **14**, and the TGA curves of polymers **13** and **14**. This material is available free of charge via the Internet at http://pubs.acs.org.

References and Notes

(1) (a) Shirakawa, H.; Louis, E. J.; MacDiarmid, A. G.; Chiang, C. K.; Heeger, A. J. *J. Chem. Soc., Chem. Commun.* **1977**, 578. (b) Chiang, C. K.; Fischer, C. R.; Park, Y. W.; Heeger, A. J.; Shirakawa, H.; Louis, E. J.; Gau, S. C.; MacDiarmid, A. G. *Phys. Rev. Lett.* **1977**, *39*, 1098. (c) Chiang, C. K.; Druy, M. A.; Gau, S. C.; Heeger, A. J.; Louis, E. J.; MacDiarmid, A. G.; Park, Y. W.; Shirakawa, H. *J. Am. Chem. Soc.* **1978**, *100*, 1013. (d) McGehee, M. D.; Heeger, A. J. *Adv. Mater.* **2000**, *12*, 1655.

(2) Kraft, A.; Grimsdale, A. C.; Holmes, A. B. *Angew. Chem.* **1998**, *110*, 416.

(3) (a) *Handbook of Conducting Polymers*, 2nd ed.; Skotheim, T. J., Elsenbaumer, R. L., Reynolds, J. R., Eds.; Dekker: New York, 1998. (b) *Semiconducting Polymers: Chemistry, Physics and Engineering*, 1st ed.; Hadziioannou, G., van Hutten, P. F., Eds.; Wiley-VCH: Weinhem, Germany, 2000.

(4) Bunz, U. H. F. *Chem. Rev.* **2000**, *100*, 1605.

(5) Scherf, U.; List, E. J. W. *Adv. Mater.* **2002**, *14*, 477.

(6) Burroughes, J. H.; Bradley, D. D. C.; Brown, A. R.; Marks, R. N.; MacKays, K.; Friend, R. H.; Burn, P. L.; Holmes, A. B. *Nature (London)* **1990**, *347*, 539.

(7) Hörhold, H.-H.; Helbig, M. *Makromol. Chem., Macromol. Symp.* **1987**, *12*, 229.

(8) Greenham, N. C.; Moratti, S. C.; Bradley, D. D. C.; Friend, R. H.; Holmes, A. B. *Nature (London)* **1993**, *365*, 628.

(9) Pinto, M. R.; Hu, B.; Karasz, F. E.; Akcelrud, L. *Polymer* **2000**, *41*, 2603.

(10) (a) Liu, M. S.; Jiang, X.; Liu, S.; Herguth, P.; Jen, A. K. Y. *Macromolecules* **2002**, *35*, 3532. (b) Krebs, F. C.; Jørgensen, M. *Macromolecules* **2000**, *35*, 7200.

(11) Lux, A.; Holmes, A. B.; Cervini, R.; Davies, J. E.; Moratti, S. C.; Grüner, J.; Cacialli, F.; Friend, R. H. *Synth. Met.* **1997**, *84*, 293.

(12) Chen, Z.-K.; Meng, H.; Lai, Y.-Hing, Huang, W. *Macromolecules* **1999**, *32*, 4351.

(13) (a) Marsella, M. J.; Fu, D. K.; Swager, T. M. *Adv. Mater.* **1995**, *7*, 145. (b) Gillissen, S.; Jonforsen, M.; Kesters, E.; Johansson, T.; Theander, M.; Andersson, M. R.; Inganäs, O.; Lutsen, L.; Vanderzande, D. *Macromolecules* **2001**, *34*, 7294.

(14) (a) Egbe, D. A. M.; Tillmann, H.; Birckner, E.; Klemm, E. *Macromol. Chem. Phys.* **2001**, *202*, 2712. (b) Egbe, D. A. M.; Roll, C. P.; Klemm, E. *Des. Monomers Polym.* **2002**, *5*, 245. (c) Egbe, D. A. M.; Roll, C. P.; Birckner, E.; Grummt, U.-W.; Stockmann, R.; Klemm, E. *Macromolecules* **2002**, *35*, 3825. (d) Egbe, D. A. M.; Birckner, E.; Klemm, E. *J. Polym. Sci., Part A: Polym. Chem.* **2002**, *40*, 2670.

(15) (a) Brizius, G.; Pschirer, N. G.; Steffen, W.; Stitzer, K.; zur Loye, H.-C.; Bunz, U. H. F. *J. Am. Chem. Soc.* **2000**, *122*, 12435. (b) Ramos, A. M.; Rispens, M. T.; van Duren, J. K. J.; Hummelen, J. C.; Janssen, R. A. J. *J. Am. Chem. Soc.* **2001**,

123, 6714. (c) Schenning, A. P. H.; Tsipis, A. C.; Meskers, S. C. J.; Beljonne, D.; Meijer, E. W.; Brédas, J. L. *Chem. Mater.* **2002**, *14*, 1362. (d) Wilson, J. N.; Windscheif, P. M.; Evans, U.; Myrick, M. L.; Bunz, U. H. F. *Macromolecules* **2002**, *35*, 8681.
(16) (a) Kaufman, J. H.; Chung, T.-C.; Heeger, A. J. *Solid State Commun.* **1983**, *47*, 585. (b) Kaufman, J. H.; Chung, T.-C.; Heeger, A. J. *J. Electrochem. Soc.* **1984**, *131*, 2847. (c) Kaner, R. B.; Porter, S. J.; Nairns, D. P.; MacDiarmid, A. G. *J. Chem. Phys.* **1989**, *90*, 1303.
(17) Demas, J. N.; Crosby, G. A. *J. Phys. Chem.* **1971**, *75*, 991.
(18) Teuschel, A. Ph.D. Thesis, Jena, 1997.
(19) Egbe, D. A. M.; Klemm, E. *Macromol. Chem. Phys.* **1998**, *199*, 2683.
(20) Weder, C.; Wrighton, M. S. *Macromolecules* **1996**, *26*, 5157.
(21) Jones, S.; Atherton, J. C. C. *Synth. Commun.* **2001**, *31*, 1799.
(22) Meier, H.; Aust, H. *J. Prakt. Chem.* **1999**, *341*, 466.
(23) (a) Dieck, H. A.; Heck, F. H. *J. Org. Chem.* **1975**, *93*, 259. (b) Tohda, Y.; Sonogashira, K.; Hagihara, N. *Tetrahedron Lett.* **1975**, *50*, 4467. (c) Yamamoto, T.; Yamamoto, A. *Bull. Chem. Soc. Jpn.* **1984**, *57*, 752. (d) Yamamoto, T. *Bull. Chem. Soc. Jpn.* **1999**, *72*, 621.
(24) (a) Wadsworth, W. S. *Org. React.* **1977**, *25*, 73. (b) Hörhold, H.-H.; Opfermann, J. *Makromol. Chem.* **1970**, *131*, 105.
(25) Mühlbacher, D. Diploma thesis, Linz, Austria, 2002.
(26) (a) Nguyen, T.; Doan, V.; Schwartz, B. J. *J. Chem. Phys.* **1999**, *110*, 4068. (b) Nguyen, T.; Martini, I. B.; Liu, J.; Schwartz, B. J. *J. Phys. Chem. B* **2000**, *104*, 237.
(27) Chen, Z.-K.; Huang, W.; Wang, L.-H.; Kang, E.-T.; Chen, B. J.; Lee, C. S.; Lee, S. T. *Macromolecules* **2000**, *33*, 9015.
(28) (a) Bredas, J. L.; Silbey, R.; Boudreux, D. S.; Chance, R. R. *J. Am. Chem. Soc.* **1983**, *105*, 6555. (b) deLeeuw, D. M.; Simenon, M. M. J.; Brown, A. B.; Einerhand, R. E. F. *Synth. Met.* **1997**, *87*, 53.
(29) (a) Liu, M. S.; Jiang, X.; Liu, S.; Herguth, P.; Jen, A. K.-Y. *Macromolecules* **2002**, *35*, 3532. (b) Liu, Y.; Liu, M. S.; Jen, A. K.-Y. *Acta Polym.* **1999**, *50*, 105.
(30) Gerischer, H., Tobias, C. W., Eds. *Advances in Electrochemistry and Electrochemical Engineering;* John Wiley: New York, 1977; Vol. 10, p 213.
(31) (a) Gomer, R. J.; Tryson, G. *J. Chem. Phys.* **1977**, *66*, 4413. (b) Kötz, R.; Neff, H.; Müller, K. *J. Electroanal. Chem.* **1986**, *215*, 331.
(32) Pfeiffer, S.; Hörhold, H.-H. *Macromol. Chem. Phys.* **1999**, *200*, 1870.
(33) Volta, S. Ph.D. Thesis, Jena, 2002.
(34) (a) Hwang, S.-W.; Chen, Y. *Macromolecules* **2001**, *34*, 2981. (b) Hwang, S.-W.; Chen, Y. *Macromolecules* **2002**, *35*, 5438.

MA0301395